

Comparative luminescent analysis of healthy and calcified arteries for catheter guidance in chronic total occlusion revascularization

Ludmila Bakueva^{1,5,*}, Nigel Munce^{1,5}, Lukasz Brzozowski^{1,5},
Ivan Gorelikov^{1,5}, John J. Graham^{2,5}, Brian K. Courtney^{3,5},
Stephen E. Fremes⁴, Graham A. Wright^{1,5}, and John A. Rowlands^{1,5}

¹*Department of Medical Biophysics, University of Toronto*

²*Department of Cardiology, University of Toronto*

³*Department of Medicine, University of Toronto*

⁴*Division of Cardiovascular Surgery, University of Toronto*

⁵*Imaging Research, Sunnybrook Health Sciences Centre,
2075 Bayview Avenue, Toronto M4N 3M5, Canada*

**Corresponding author: bakueva@sten.sunnybrook.utoronto.ca*

Received 24 April 2006, accepted 31 July 2006

Abstract

The work is devoted to photoluminescence investigation of arterial walls in order to create a new navigation method for minimally invasive treatment of cardiovascular disease in the presence of chronic total occlusions. The comparative analysis of luminescent spectra for healthy and calcified arterial tissue was realized in two types of investigations: integral spectral measurements of the samples and spectroscopic imaging with a laser confocal microscope. In both cases qualitative features in spectra are revealed that could be used for discrimination between the arterial wall and chronic total occlusion. Further increase in sensitivity and reliability of the method was shown to be achieved by treating the sample by a solution of semiconductor nanocrystals with high luminescent efficiency.

1 Introduction

Treatment of cardiovascular disease can be carried out either through surgery or minimally invasive interventions by performing percutaneous transluminal angioplasty (PCTA). PCTA treatment of stenotic coronary and peripheral artery lesions has become a well accepted therapy. Percutaneous methods are often cheaper and faster than the surgical approaches and can result in reduced trauma to the patient, a lower number of early complications, and more rapid recovery.

Until recently, the restenosis of treated lesions has been considered the main weakness of PCTA treatment. With the advent of drug eluting stents that effectively prevent restenosis, this problem has diminished dramatically. Currently the leading contraindication to PCTA is the presence of chronic total occlusions (CTOs) on the diagnostic angiogram [1, 2]. CTO is defined as an arterial occlusion that is at least three months old and that displays no flow of the contrast agent on the angiogram [3, 4].

Despite many advances, percutaneous treatment of CTOs still suffers from a relatively low success rate. Although CTOs are present in about one third of coronary angiograms [5, 6], the recanalization of CTO constitutes only 5% to 20% of all PCTA procedures [1, 4, 7]. The success rate of these procedures is around 60% to 70% [1, 4]. However the majority of these cases is simply not attempted and is treated surgically. A large part of the inherent difficulty in treating CTOs is the poor navigation capabilities during the recanalization of tortuous vessels.

Imaging and navigation during the PCTA of CTO are currently performed using x-ray contrast angiography for visualization of flow through the lumen of the artery. As angiographic contrast agent cannot enter occluded regions, navigation of catheters and guide wires during interventions becomes difficult, resulting in increased risk of vessel perforation. A brief outline follows on technologies currently in use to aid navigation.

Magnetic Resonance Imaging (MRI) can potentially aid navigation during PCTA of CTOs. MRI has recently been used to visualize thrombus, and distinguish it from the vessel wall of carotid arteries in swine [8]. However, motion artifacts due to the cardiac cycle make high-resolution imaging of coronary arteries difficult. Interventional MRI also suffers from a scarcity of available scanners and MRI-compatible devices along with high procedural costs. Finally, many cardiac patients have pacemakers or other implants that are not compatible with MRI.

Raman Scattering Spectroscopy can precisely determine the composition of the illuminated material, and hence potentially distinguish between signal

from the plaque and that of a vessel wall [9, 10]. The Raman signal is however very weak, which poses a problem in PCTA techniques where the need for long fiber optic catheters will result in a significant optical reducing the signal.

Optical Coherence Reflectometry (OCR) [4] is a promising technology to increase the navigation capabilities of CTOs during PCTA. OCR uses the principle of light interference to analyze the medium along a single straight line in front of the fiber optic catheter. The reflected wavefront is monitored for spikes in the reflectivity, which signifies proximity to the vessel wall. While OCR has demonstrated promising results, there are problems associated with this technique. A given occlusion can be composed of highly organized plaque with calcifications. Such calcifications can be more reflective than the vessel wall, thus complicating the analysis of the optical signal. Beating heart and breathing motion can introduce further errors.

Given the need for better navigation during PCTA treatment of CTOs, we analyze below a new solution to address this problem by using the distinct photoluminescent properties of arterial walls and CTO plaques to enhance guidance during minimally invasive CTO revascularization. In this technique, a fiber optic equipped catheter would be used as the excitation and collection optical probe during the debulking of a CTO. The spectral characteristics of the collected signal would be analyzed and the interventionalist would be alerted when the probe was in contact with the vessel wall. This method, if feasible, would permit the intraprocedural navigation of the debulking catheter at a level which is not provided by any other currently available method. To demonstrate the feasibility of this technique we have examined the photoluminescent properties of arterial wall and CTO plaque samples and show that they are distinguishable and repeatable. Further improvement of this technique could be achieved by using semiconductor nanocrystals characterized by a very high quantum yield of photoluminescence.

2 Morphology of CTO and healthy arterial samples

2.1 Pre-operative contrast X-ray angiography and initial sample preparation

The samples analyzed were obtained from human legs that were amputated for standard clinical indications, including foot ischemia and its associated

complications. The study protocol was approved by the Research Ethics Board of the Sunnybrook Health Sciences Centre, and written informed consent for this study was obtained from all patients. During this pilot study we have harvested arterial samples from eight patients. The vessels examined included the major arteries of the calf region: anterior tibial arteries (ATA) and posterior tibial arteries (PTA).

The presence of a CTO, as confirmed by a pre-operative angiogram or as expected from the patient's history of critical lower limb ischemia, was used as a screening criterion for inclusion in our study. The diameter of the original vessels was between 3 and 6 mm, with a range of wall thicknesses between 300 and 800 μm .

With the account of preliminary angiographic investigations, two groups of samples were selected: i) healthy arteries; ii) arteries with CTO. Micro-computed tomography was conducted to further determine the morphology of the occluded samples [11].

To reconfirm the proper choice of the samples, some were taken for independent histological analysis described below in Sec.IIB. The samples were rinsed in saline, after which the parts of these vessels (7-10mm length) were opened longitudinally for further fluorescence measurements. Besides the two above-mentioned types of artery segments, for some specific measurements we also prepared calcified formations separated from the arteries tissue.

2.2 Histology

Histological analysis was performed on the axial cross-sections prepared from a subset of CTO samples and healthy samples. The perfusion-fixed arteries were prepared using standard paraffin-embedding techniques. Cross-sections were taken at locations both proximal to and within the CTOs, and at representative locations along the healthy arterial segments. The arteries were subsequently stained using H&E and Masson's Trichrome stains.

Representative histology is shown in Fig. 1. H&E staining in Figs. 1a and 1c demonstrates cellular elements, while Masson's Trichrome staining in Figs. 1b and 1d highlights the extent of connective tissue components with collagen and extracellular matrix appearing in blue; smooth muscle and cytoplasmic elements appear in red. Figs. 1c, 1d demonstrate a relatively healthy arterial cross-section with mild eccentric thickening of the intimal layer. While the intima and media layers of the vessel walls contain a moderate concentration of organized collagen, the wall contains a higher concentration of cellular components than the intraluminal cores of

the CTO cross-sections. Figs. 1a, 1b are cross-sections of a CTO. The Masson's Trichrome stained section demonstrates a lack of cellularity and a higher concentration of disorganized collagen within the luminal cores of the CTOs compared with the surrounding walls of both the healthy samples and the CTO cross-sections.

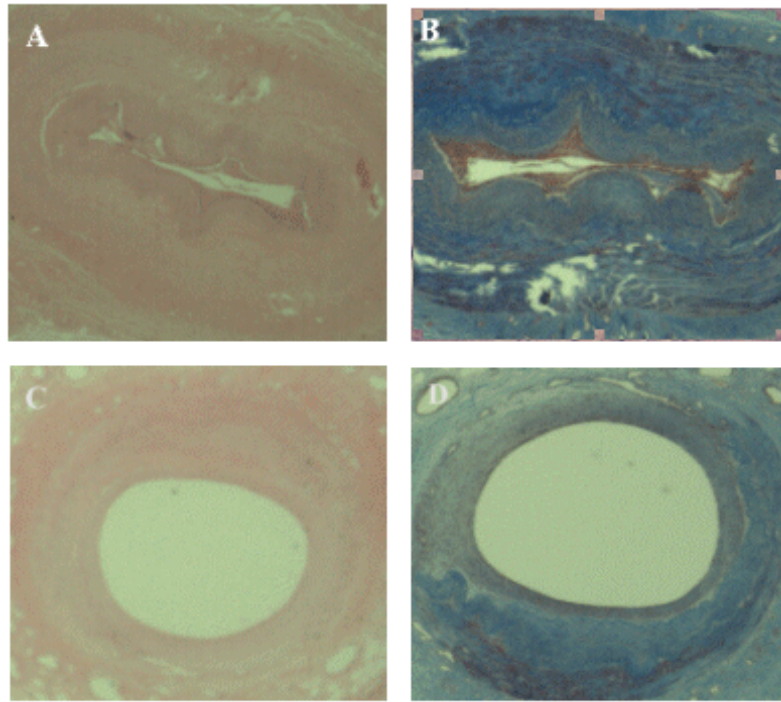


Figure 1: Histology results from two arterial samples. Fig.1a, 1b show a CTO sample, while 1c, 1d depict a relatively healthy artery. Using the comparison with relatively healthy arteries, it is possible to distinguish the CTO lumen from the vessel wall. H&E staining (1a, 1c) shows that the lumen CTO is made up out of dense fibrous tissue. Masson's Trichrome (1b, 1d) suggests that the fibrous material is made mainly of a collagen.

CTOs may display a large degree of variation in their plaque constituents and density. Typically, CTOs may contain lipid, calcium, and collagen. The etiology of these differences in CTO configurations and the factors that influence their development are not known at present. Despite these differences in configuration, it appears as though the higher concentration of collagen

and lower degree of cellularity is consistent within the relatively small number of samples examined in this pilot study. These representative features were shared by all the healthy and CTO plaque samples analyzed. Based on this evidence we find it appropriate to consider such composition as representative of a CTO in ATA or PTA. This is further supported by the repeatability of the luminescence results described in the following section.

In addition, since the vessel wall of the occluded samples appears to have preserved its composition and integrity, we find it justified to assume that the luminescence signal from the arterial wall within the CTO will be very similar to the luminescence signal of a healthy arterial wall.

3 Luminescence properties of occluded and healthy arterial samples

The samples described in the previous section were subjected to two types of luminescent investigations: integral spectral measurements of the samples and spectroscopic imaging with a laser scanning confocal microscope.

For the first type of measurements, all the samples were cut longitudinally and spread along the incision, exposing the inside of the sample (which was either CTO plaque or the healthy arterial wall). The samples were placed in a specially prepared compartment that permitted repeatable measurement of the emitted light. The illuminated surface area of spread samples was approximately $2 \times 5 \text{ mm}^2$. The measurements were carried out using the Photon Technology International Spectrophotometer C-60 with an arc lamp light source. This system permits emission and excitation spectra analysis in the spectral range 200 to 900 nm. The excitation beam was directed onto the samples at a 45° angle, and the light emitted from the sample was collected along the direction normal to the sample surface.

The absolute value of luminescence intensity depends on the sample volume, the illuminated sample area, and the excitation and collection efficiencies. As such, the absolute collected signal intensity can vary among the samples of very similar composition, especially during the revascularization where heart and breathing motions that result in catheter movement cannot be fully eliminated. We therefore analyzed the luminescence spectra obtained using relative (normalized to the long wavelength maximum intensity) rather than absolute measurements. In our analysis we identified several of the quantitative spectral features which were: i) wavelength of luminescence maxima; ii) spectral separation between maxima; iii) relative intensities of different maxima in normalized spectra; iv) differential spectra

obtained by subtraction of the normalized healthy artery luminescence spectra from the normalized CTO spectra; and v) variation of these parameters with the excitation wavelength.

In most biological media (contrary to, say, semiconductor crystals) excited states created by optical pumping do not reach quasi-equilibrium prior to emitting light. As a result, luminescence spectra may depend on the excitation wavelength and this dependence provides additional information on the object. We therefore investigated spectra at two different excitation wavelengths, 300 nm and 340 nm, in order to gain more information on the photoluminescence characteristics of healthy and CTO plaque samples. These wavelengths are close to the laser wavelengths 308 nm and 337 nm widely used in medical applications, which may simplify corresponding equipment. The 308 nm excimer laser is applied in angioplasty [12] while the nitrogen 337 nm laser is of common use in the medical investigation of malignant cancer tissue [13,14].

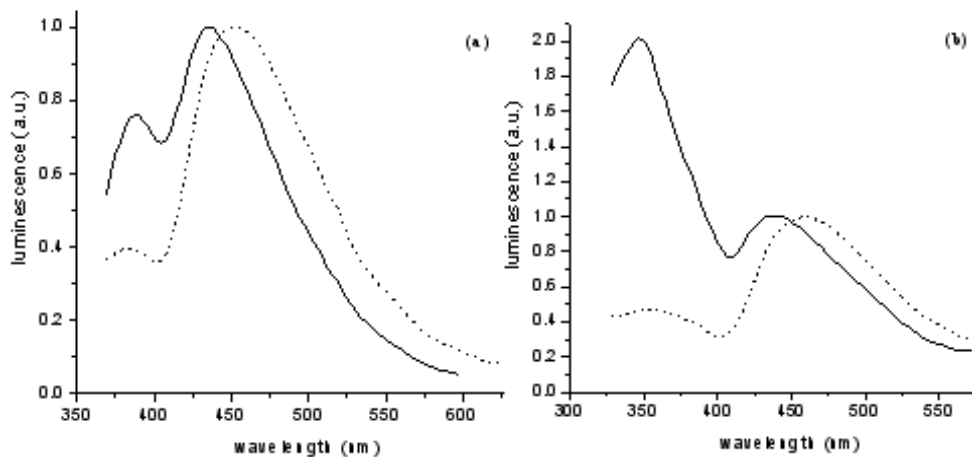


Figure 2: Normalized photoluminescence spectra of the healthy (dashed line) and the CTO plaque tissue (solid line) at the excitation wavelengths a) 340 nm, b) 300 nm.

Fig. 2a shows typical luminescence spectra of a healthy artery (dashed line) and CTO plaque (solid line) in the 360-600 nm spectral region when excited at 340 nm. Both curves are characterized by two distinct spectral peaks, with the long-wavelength (LW) peak having a greater amplitude than the short-wavelength (SW) peak. The amplitude ratio LW/SW is much

larger in the healthy sample than in the CTO-sample (2.5 compared to 1.32), which is the first feature that can be used to discriminate between these two sample groups. The second feature is the difference in positions of the LW peak, which in CTO tissue appears to be shifted by 20-25 nm towards shorter wavelengths relative to the LW peak of the healthy tissue.

Qualitatively, such bimodal luminescence spectra have been recorded by a number of authors [15-18]. Distinctions between the solid and dashed curves can be explained by the fact that the structural protein collagen, an essential component of atherosclerotic plaques, is characterized by the intensive luminescence band in the region 350-390 nm [18, 19] corresponding to our SW peak.

A more noticeable difference between healthy and CTO plaque arterial samples is detected when the excitation frequency is shifted from 340 to 300 nm (Fig. 2b). This causes a relative increase of the SW peak amplitude in both groups of samples. While in healthy samples this increase is only several percent, in CTO-samples we have a complete inversion of relative intensities – the initially lower SW peak becomes twice as high as the LW peak. The 20-25 nm difference in the position of the LW peak is conserved for the 300 nm excitation frequency as well.

Our explanation for this sharp increase of the SW peak in CTO plaque samples accompanying the decrease in of the excitation wavelength is that it is connected with the higher concentration of collagen in CTO plaque compared to that in the healthy arterial wall. According to [20,21], collagen has strong optical absorption in the spectral region 300-340 nm which means that switching from 340 to 300 nm excitation is accompanied by an increase in the number of molecules in the excited state and, hence, effectively an increase in the recombination (part of which is a radiative recombination) in the CTO plaque.

We have verified that our luminescence results are highly repeatable. We analyzed 12 samples from each group (healthy and CTO arteries) and all normalized results were within 10% of the average values for their respective groups.

To conduct laser scanning microscopy of healthy and occluded arteries, thin (about 2 mm) perpendicular slices were prepared and fixed at the cover slip glasses. For control comparative measurements, some calcified formations were detached from arterial walls and placed separately at the cover slip glasses. All measurements were performed using a Zeiss LSM 510 META point scanning laser confocal microscope using excitation by an Ar laser ($\lambda = 458$ nm). The microscope allowed for local spectroscopic imaging in the spectral region 480-700 nm by using a 32-element PMT and a grating.

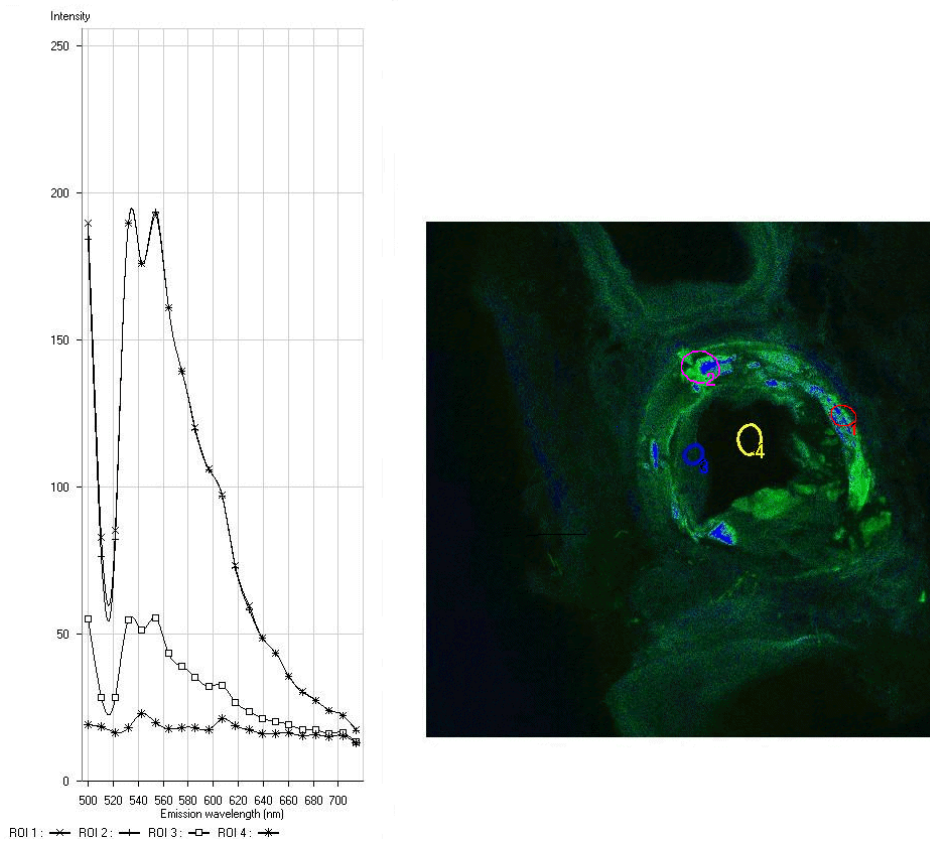


Figure 3: Microscopic image of a cross-section of artery (right) and local luminescent spectra (left) of detailed regions.

Fig. 3 demonstrates the cross-sectional microscopic image of an artery containing calcified formations appearing as highly reflective regions. The left side of the figure contains the emission spectra taken from two regions (#1 and #2) belonging to well-developed calcified formations, from the region (#3) corresponding to the intimal area and from the lumen region (#4). The first two contain a characteristic structure consisting of two close peaks at 530 and 550 nm. This coincidence of the spectra measured at two different points indicates that the mentioned spectral structure is a characteristic of highly organized collagen, rather than some artifact. The #3 spectrum is characterized by the same spectral features but with essentially lower amplitude, while the last curve is much less intense and contains no

distinctive structure. Thus our conclusions agree with those shown in Fig. 2: the healthy and atherosclerotic regions are characterized by qualitatively similar features of the luminescence spectrum but with essentially different quantitative parameters.

Note that these results are obtained for excitation by visible light, not exciting the two characteristic peaks shown in Fig. 2. Hence the data of Fig. 3 do not contradict those of Fig. 2 but, belonging to another spectral region, complement them indicating one more noticeable distinction between the luminescence spectra of healthy and atherosclerotic calcified arteries.

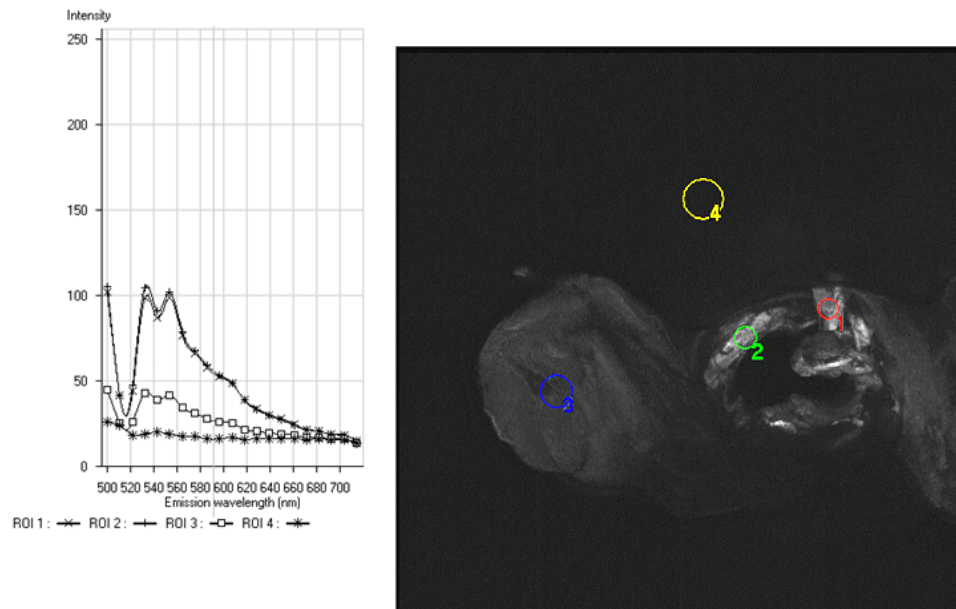


Figure 4: Microscopic image of a calcified formation (right) and local luminescent spectra (left) of detailed regions.

For comparison, we also performed a microscopic investigation of calcified formations detached from the arterial walls. A typical result is presented in Fig. 4 where the regions #1 and #2, on the one hand and #3 (mostly fat tissue), on the other hand, correspond to formations of different shape, surface quality, and homogeneity. For this reason, absolute intensity of

their luminescence is, naturally, different but has similar spectral structure, which, in turn, coincides with the structure in Fig. 3. Thus we may claim that this spectral structure is characteristic to the atherosclerotic material, rather than to healthy artery walls and agrees with the fact that in Fig. 3 the intensity of these peaks is much higher in sclerotic than in healthy regions.

4 Semiconductor nanocrystals in CTO diagnostics

The results of the previous section, as well as relevant data of other authors [15-19, 21] demonstrate that in principle it is possible to design a catheter guidance system using comparative luminescence analysis of CTO plaques in comparison with healthy arterial walls. Practical application of this method in vivo requires further increases in sensitivity and reliability of this luminescence-based tissue differentiation. It can be done by using semiconductor nanocrystals (NC) which in recent years have found a number of promising applications in biomedical imaging [22, 23].

For our investigation, we used colloidal core-shell CdSe/ZnS NC synthesized using air stable reagents with CdO and ZnO as precursors. The fabrication technology included also a subsequent ligand exchange at the NC surface, which is very important for transforming NC in organic solvent into a water-soluble system compatible with biological assays, and is described in more detail in [24]. The particular ligand used in the present work was dihydrolipoic acid (DHLA) providing NC with hydrophilic properties. Among all hydrophilic ligands, DHLA-capped NC are the most stable in water solution due to the presence of two S atoms providing denser coverage of the NC surface.

NCs had a diameter of 4 nm and were characterized by a relatively narrow photoluminescence line $\lambda \cong 582$ nm with FWHM 35 nm. This line is far from the described above spectral peaks of NC-free objects so that the results given below do not interfere with those of Sect. 3 but simply supplement them with an additional diagnostic instrument.

To embed NC into the samples, 0.1 μ M solution of NC was dropped onto the artery surface and after 5 min. of wetting, the sample was mounted on the microscope holder. Fig. 5 demonstrates the cross-section of an artery containing calcified formations. The object is similar to that in Fig. 3 but the image has a rather different appearance. While in Fig. 3 the plaque regions look bright, in Fig.5 they are dark but with a well-developed bright contour. This is due to the fact that NC are concentrated mostly outside

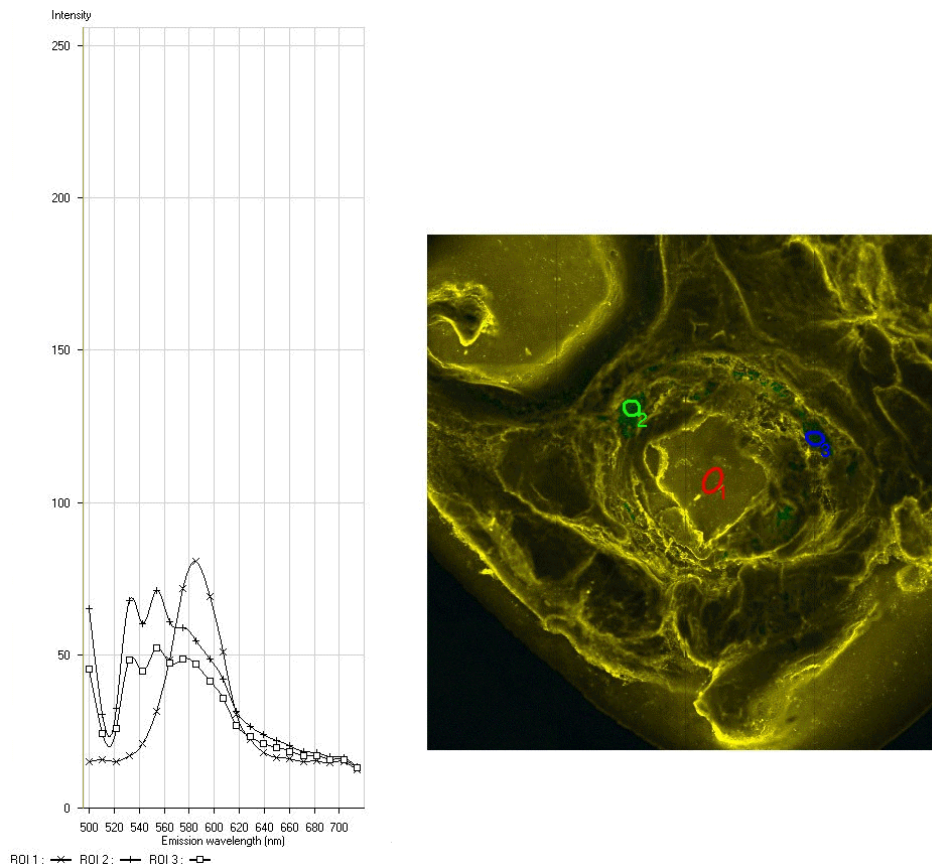


Figure 5: Microscopic image of a cross-section of artery with embedded NC (right) and local luminescent spectra (left) of detailed regions.

these regions, presumably due to a difference in wettability. As a result, the presence of NC additionally highlights interfaces between different types of tissues. Note that such selective distribution of NC is obtained without NC conjugation to some particular biomolecules for a specific targeting typically used in NC-based imaging.

We have chosen three regions of interest in Fig. 5: the picture: #1 – lumen of the artery, #2 – region with calcification in a medial wall, and #3 – region with connective tissue and calcification formation. In the #1 region, the luminescence spectrum shown in the left side of the figure contains only the line of NC emission. The spectra of the two other regions contain a

superposition of a bimodal spectrum with the maxima at 530 and 550 nm observed in such regions in the absence of NC (see Fig.3) and a small peak (or a shoulder) related to NC.

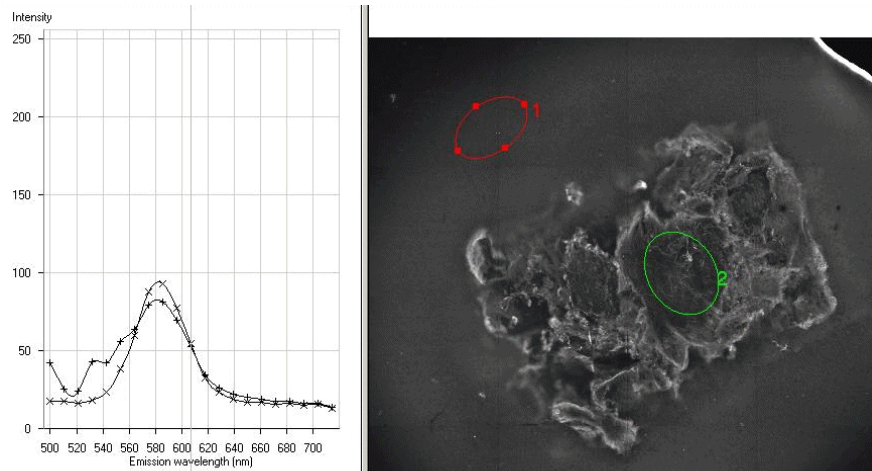


Figure 6: Microscopic image of a calcified formation with embedded NC (right) and local luminescent spectra (left) of detailed regions.

Fig. 6 shows the microscopic image of a detached calcified formation (similar to Fig. 4) treated with a NC-containing solution. Control spectral measurements outside the formation (#1) demonstrate the only maximum corresponding to NC luminescence. At the same time, the spectrum from the #2 region contains the already described spectral doublet with the maxima at 530 and 550 nm. However, contrary to Fig. 5 where the doublet structure dominated over the NC peak, in the last case it is noticeably weaker. Thus the picture confirms the main conclusion mentioned previously: regions with different degrees of calcification have the same structure of luminescent peaks but their relative intensities differ dramatically and this can be used for diagnostic properties.

5 Conclusions

We have demonstrated that the analysis of photoluminescence spectra provides a promising approach to permit the discrimination between human arterial walls and CTO plaque. Prior to photoluminescence measurements,

we conducted angiography which confirmed the occluded or healthy nature of specimens. Our understanding of morphology and composition of CTOs was furthered by performing a preliminary analysis of such lesions using histological techniques.

The photoluminescence spectra of all investigated samples had two maxima, whose spectral position and relative intensity depended on the sample group (arterial wall vs. CTO plaque) and excitation wavelength. Thus a quite simple instant analysis of the spectra allows one to discriminate between the arterial wall and CTO plaque thus giving the interventionalist the information necessary to enable safe catheter navigation through these otherwise challenging lesions.

Further work in this direction must include, in particular, the investigation of possible difference in photoluminescence properties of the peripheral and coronary occlusions and vessel walls, as well as the analysis of whether the photoluminescence properties of the samples were affected by environmental factors such as temperature, sample preparation, time from harvesting.

We thank Alexander Dick, Bradley Strauss, Beiping Qiang, Elena Encioiu, Jagdish Butany, and Ulrich Krull for useful discussions and help in the preparation of our experiments.

References

- [1] J.A. Puma, M.H. Sketch, Jr., J.E. Tchong, R.A. Harrington, H.R. Phillips, R.S. Stack, and R.M. Califf, *J. Am. Coll. Cardiol.* **26**, 1 (1995).
- [2] S.S. Srivatsa, W.D. Edwards, C.M. Boos, D.E. Grill, G.M. Sangiorgi, K.N. Garratt, R.S. Schwartz, and D.R. Holmes, Jr., *J. Am. Coll. Cardiol.* **29**, 955 (1997).
- [3] D.G. Sionis, V.A. Tolis, and L.K. Michalis, *Hellenic Journal of Cardiology* **44**, 136 (2003).
- [4] H. Cordero, K.D. Warburton, P.L. Underwood, and R.R. Heuser, *Catheter Cardiovasc. Interv.* **54**, 180 (2001).
- [5] E. Delacretaz and B. Meier, *Am. J. Cardiol.* **79**, 185 (1997).
- [6] J.N. Hamburger, G.H. Gijssbers, Y. Ozaki, P.N. Ruygrok, P.J. de Feyter, and P.W. Serruys, *J. Am. Coll. Cardiol.* **30**, 649 (1997).

- [7] K.W. Lau, Z.P. Ding, U. Sigwart, and L. Lam, *Singapore Med. J.* **41**, 468 (2000).
- [8] R. Corti, J.I. Osende, Z.A. Fayad, J.T. Fallon, V. Fuster, G. Mizsei, E. Dickstein, B. Drayer, and J.J. Badimon, *J. Am. Coll. Cardiol.* **39**, 1366 (2002).
- [9] H.P. Buschman, E.T. Marple, M.L. Wach, B. Bennett, T.C. Schut, H.A. Bruining, A.V. Brusckke, A. van der Laarse, and G.J. Puppels, *Anal. Chem.* **72**, 3771 (2000).
- [10] T.J. Romer, J.F. Brennan, 3rd, G.J. Puppels, A.H. Zwinderman, S.G. van Duinen, A. van der Laarse, A.F. van der Steen, N.A. Bom, and A.V. Brusckke, *Arterioscler. Thromb. Vasc. Biol.* **20**, 478 (2000).
- [11] L. Bakueva, L. Brozowski, B. Courtney, N. Reznik, S.E. Fremes, and J.A. Rowlands, *Proc of SPIE, Photonics North Symposium* **5969**, 271 (2005).
- [12] O. Topaz, R. Lippincott, J. Bellendir, K. Taylor, and C. Reiser, *J. Clin. Laser Med. Surg.* **19**, 9 (2001).
- [13] N. Ramanujam, M.F. Mitchell, A. Mahadevan, S. Warren, S. Thomsen, E. Silva, and R. Richards-Kortum, *Proc. Natl. Acad. Sci. USA* **91**, 10193 (1994).
- [14] S.O. Lim, S.J. Park, W. Kim, S.G. Park, H.J. Kim, Y.I. Kim, T.S. Sohn, J.H. Noh, and G. Jung, *Biochem. Biophys. Res. Commun.* **291**, 1031 (2002).
- [15] F.W. Cutruzzola, M.L. Stetz, K.M. O'Brien, G.R. Gindi, L.I. Laifer, T.J. Garrand, and L.I. Deckelbaum, *Lasers in Surgery and Medicine* **9**, 109 (1989).
- [16] S. Andersson-Engels, J. Johansson, and S. Svanberg, *Spectrochimica Acta A* **46**, 1203 (1990).
- [17] L. Marcu, M.C. Fishbein, J.-M.I. Maarek, and W.S. Grundfest, *Arterioscler. Thromb. Vasc. Biol.* **21**, 1244 (2001).
- [18] L. Marcu, Q. Fang, J.A. Jo, T. Papaioannou, A. Dorafshar, T. Reil, J.-H. Qiao, J.D. Baker, J.A. Freischlag, and M.C. Fishbein, *Atherosclerosis* **181**, 295 (2005).

- [19] J.J. Baraga, R.P. Rava, P. Taroni, C. Kittrell, M. Fitzmaurice, and M.S. Feld, *Lasers in Surgery and Medicine* **10**, 245 (1990).
- [20] N. Ramanujam, *Fluorescence Spectroscopy In Vivo* (J. Wiley & Sons, 1995).
- [21] T.G. Papazoglou, *J. Photochem. Photobiol. B* **28**, 3 (1995).
- [22] X.Michalet, F. Pinaud, T.D. Lacoste, M. Dahan, M.P. Bruchez, A.P. Alivisatos, and S. Weiss, *Single Mol.* **2**, 261 (2001).
- [23] W.J. Parak, D. Gerion, T. Pellegrino, D. Zanchet, M. Micheel, S.C. Williams, R. Boudreau, M.A. Le Gros, C.A. Larabell, and A.P. Alivisatos, *Nanotechnology* **14**, R15 (2003).
- [24] E. Bogdanovic, L. Bakueva, L. Brzozowski, I. Gorelikov, D.J. Dumont, and J.A. Rowlands, *Proc. of SPIE, Photonics North Symposium* **5969**, 1 (2005).